ASSOCIAÇÃO PORTUGUESA DOS RECURSOS HÍDRICOS

Journal of Integrated Coastal Zone Management (2023) 23(1): 27-40
© 2023 APRH
ISSN 1646-8872
DOI 10.5894/rgci-n499
url: https://www.aprh.pt/rgci/rgci-n499.html

AN ASSESSMENT OF RELATIVE POTENTIAL IMPACTS TO CYPRUS' SHORELINE DUE TO OIL SPILLS IN THE EASTERN MEDITERRANEAN SEA

Nikolas Gomes Silveira de Souza[@ 1], Jader Lugon Jr.[1, 2], Edna N. Yamasaki[3], Ioannis Kyriakides[4], Antônio J. Silva Neto[5]

ABSTRACT: An oil spill occurrence is a concerning pervasive situation that can result in significant risk, depending on where it starts, the oil properties, and the environmental conditions. In the region of Cyprus, there is an intense traffic of shipping activities which intensifies the risk of an oil spill due to vessel density and prolongated permanence time. The purpose of this work is to obtain the relative potential impact in Cyprus by performing an assessment based on mathematical simulations to identify the critical places in the Eastern Mediterranean Sea, aiming at increasing the readiness for minimising the impact of an oil spill in sensitive areas, with attention to the atmosphere, hydrosphere, lithosphere, biosphere, and anthroposphere. This work simulated 384 scenarios using Mohid and Opendrift platforms with the same data input. The preliminary results presented significant impact in Cyprus' western regions, mainly. However, after interpolating with history, sensitivity, distance, and two models, only three specific regions showed a potential relative impact. Though different platforms have been used, there were some equivalences in the predictions. Based on it, a new and more specific mathematical method was proposed to assess the potential relative impact of an oil spill in Cyprus, concluding that even with much more intense oil transport in other areas of the Eastern Mediterranean Sea, the most significant relative risks are in fact, in the areas surrounding Cyprus. In particular, the region in the south, east and west of Cyprus. It must be emphasised that the south of Cyprus is an important region for the economy of the country.

Keywords: Oil, Spill, Mohid, Opendrift, Risk, Assessment.

RESUMO: *Uma ocorrência de derramamento de óleo é uma situação comum e preocupante que pode resultar em um risco significante, dependendo de onde iniciou, as características do óleo e as condições ambientais. Na região do Chipre, há um intenso tráfego de atividades de transporte marítimo o qual intensifica o risco de um vazamento de óleo dada a densidade de embarcações e tempo de permanência prolongado. O objetivo deste trabalho é de se obter o impacto potencial relativo no Chipre através de uma avaliação, baseada em simulações matemáticas a fim de identificar os pontos críticos no Mar Mediterrâneo Oriental, buscando aumentar a preparação para minimização de impactos de um vazamento de óleo em áreas sensíveis, atento a temas de atmosfera, hidroesfera, litoesfera, biosfera e antroposfera. Este trabalho simulou 384 cenários usando as plataformas MOHID e Opendrift, usando os mesmos dados de entrada. Os resultados preliminares apresentaram impactos significativos à região mais oriental do Chipre, principalmente. Contudo, após interpolação com dados históricos, sensibilidade e dois modelos, apenas três regiões específicas ofereceram impacto relativo considerável. Foi observado que mesmo em diferentes plataformas, houve equivalência de resultados. Baseado nestas equivalências, um método matemático novo e mais específico foi proposto para avaliar o impacto relativo potencial de um vazamento de óleo no Chipre, concluindo que, mesmo com maior intensidade no transporte de óleo em outras áreas do Mar Mediterrâneo Oriental, os riscos relativos mais significantes foram, de fato, nas áreas próximas ao Chipre. Especificamente, na região ao sul, leste e oeste do Chipre. Deve-se esclarecer que ao sul do Chipre, há uma região importante para a economia do País.*

Palavras-chave: *Petróleo, Vazamento, Mohid, Opendrift, Risco, Avaliação.*

@ Corresponding author: nichsouz@msn.com

1 Fluminense Federal Institute (IFF-Campos), Brazil
2 Email: jlugonjr@gmail.com
3 University of Nicosia(UNIC), Cyprus. Email: yamasaki.e@unic.ac.cy
4 University of Nicosia(UNIC), Cyprus. Email: kyriakides.i@unic.ac.cy
5 Polytechnic Institute (IPRJ), Brazil. Email: ajsneto@iprj.uerj.br

Submission: 31 JAN 2022; Peer review: 10 FEB 2022; Revised: 7 SEP 2023; Accepted: 7 SEP 2023; Available on-line: 7 FEB 2024

1. INTRODUCTION

The petroleum oil spill is a major environmental problem. Despite several technological and legislative enhancements worldwide, the potential damage effects of this mineral continue to be a pervasive issue in several regions.

In the Mediterranean Sea, the accidents related to oil activities are significant (Kostianoy and Carpenter, 2018). Maritime vessel allision and collision seem to be the most common and concerning disasters in the region of the Mediterranean Sea (ITOPF, 2020). It is impossible to precisely predict the amount of oil spilled over the Mediterranean Sea, however, the literature estimates its worst-case to be round 1,000,000 tonnes of crude oil per year, not considering the intense oil spills, which are rare (Kostianoy and Carpenter, 2018). In the Eastern Mediterranean Sea, the shipping density is intense, as there are most of the exploration activities closer to this region, intensifying the potential for oil spills (Kirkos *et al*., 2018; Kostianoy and Carpenter, 2018).

This work enquiries whether an accident near and far from Cypriot shore would be a concern for the country. Spills at spots near the shoreline are expected to arrive easily and rapidly onto the shore. The farthest spills are expected to be of lower or no impact to the shore; though that could change for causes that cover the geophysical forces and anthropological activities. It is known that the lithosphere formation and water circulation in this region are complex, which makes more challenging the oil behaviour predictions (El-Geziry and Bryden, 2010; Millot and Taupier-Letage, 2005).

The Cypriot economy is highly influenced by tourism and aquaculture in coastal sites (Lemesios *et al*., 2016; Mavris, 2011). If there is an oil spill occurrence, it is likely to have strong interference in the recreational and environmental attractions of the affected regions (Ha, 2018), repealing national and international visitors (Katircioglu, 2009)this can not be said about tourism and growth or trade and tourism. This study employs the bounds test for cointegration and Granger causality tests to investigate a long-run equilibrium relationship between tourism, trade and real income growth, and the direction of causality among themselves for Cyprus. Results reveal that tourism, trade and real income growth are cointegrated; thus, a long-run equilibrium relationship can be inferred between these three variables. On the other hand, Granger causality test results suggest that real income growth stimulates growth in international trade (both exports and imports.

The aquaculture activities can be seriously compromised due to the intoxication of the organisms. The biosphere of the aquaculture regions can be affected by biochemical reactions between the oil and the local species leading it to instant death or diseases that make it inappropriate for consumption (Newman, 2015; Osuagwu and Olaifa, 2018).

Based on the preliminary expectations aforementioned, it is possible to compile a relative impact risk assessment intended to categorise more and less likely risks for an oil spill occurrence in specific spots. This analysis provides arguments to assess whether a region should be considered in an oil spill trajectory prediction.

Mathematical modelling is an increasingly used approach that allows predictions of scenarios in case of an oil spill event. Different strategies are used depending on the intention and the coverage area (Al-Rabeh *et al*., 1989; Chen *et al*., 2007; Dagestad *et al*., 2018; Silva *et al*., 2013). Occasionally, GIS (Geographical Information System) is used together with the mathematical modelling software for a georeferenced and classified map (Balogun *et al*., 2021).

Although many platforms are available to create predictions of oil spill events, they differ in programming technology and computational needs. In the present work Mohid Studio (Miranda *et al*., 2000) and Opendrift (Dagestad *et al*., 2018) platforms are used for oil spill events. Mohid is a robust FORTRAN-95 program that has been under constant development since 1985 (Neves, 1985), it covers land and sea, and has wide applicability in hydrodynamics and oil trajectory prediction. Several applications are noticed in the Mediterranean Sea, rivers, and the Atlantic Ocean (Lugon Jr. *et al*., 2020; Oliveira *et al*., 2020; Paiva *et al*., 2017).

The Opendrift package was programmed in Python platform and has been under constant development (Dagestad *et al*., 2018). This platform has wide application for ocean trajectory modelling (Dagestad *et al*., 2016). Using the Lagrangian tracking methods, it covers oil spills (Jones *et al*., 2016) and search-and-rescue applications (Ličer *et al*., 2020). Also, Opendrift has contributed to the understanding of the possible prehistoric maritime trajectories between Cyprus and other regions nearby, by simulating ocean modelling and particle tracking (Nikolaidis *et al*., 2020).

As technologies advance, computer programmes are becoming more precise in representing the various phenomena involved in a process of an oil spill. For the oil moving prediction, Mohid and Opendrift trace the oil particles using the Lagrangian transport method. This method is useful to trace each particle individually.

Several phenomena are considered in Mohid and Opendrift platforms. For a general 2D view: atmosphere winds, surface movement area, oil spreading velocity, and its evolution. For the particle: vertical oil movement, sedimentation of the oil particles, and the moment the particles reach the shoreline (beaching). For the weathering: evaporation, sedimentation, dissolution, dispersion, entrainment, emulsification, and biodegradation. Mohid could not predict the oil biodegradation, nevertheless, a new study provided a comprehensive oil spill simulation in which a new biodegradation approach was explored and presented (Li *et al*., 2017). The dissolution process is not currently covered by Opendrift (Dagestad *et al*., 2018). As the programmes differ in the mathematical approach used in its core, it is expected slight differences in the oil trajectories.

This paper presents the use of mathematical modelling to identify the potentially most critical places of the Eastern Mediterranean Sea, aiming at minimising the impact of an oil spill in the sensible areas of Cyprus.

The preliminary results could present a considerable impact in Cyprus' western regions, mainly. However, after interpolating with accident history, region sensitivity, distance to the shoreline, combining two modelling platforms, only three specific regions showed a potential relative impact.

2. STUDY AREA AND METHODOLOGY

Cyprus is an island located in the eastern part of the Mediterranean Sea. It is surrounded by several oil-gas activities, being the shipping the most notable one (Kirkos *et al*., 2018). One of the most pressing problems of this area is that the intense shipping activities give room for accidents which could lead to direct damages for Cyprus. Figure 1 presents the EMODnet projection (EMSA, 2019; Johns, 2019) for route and permanence of vessels in the study area. Accidents are not uncommon to be reported in the Eastern Mediterranean area (Kostianoy and Carpenter, 2018), as can be seen in Figure 2.

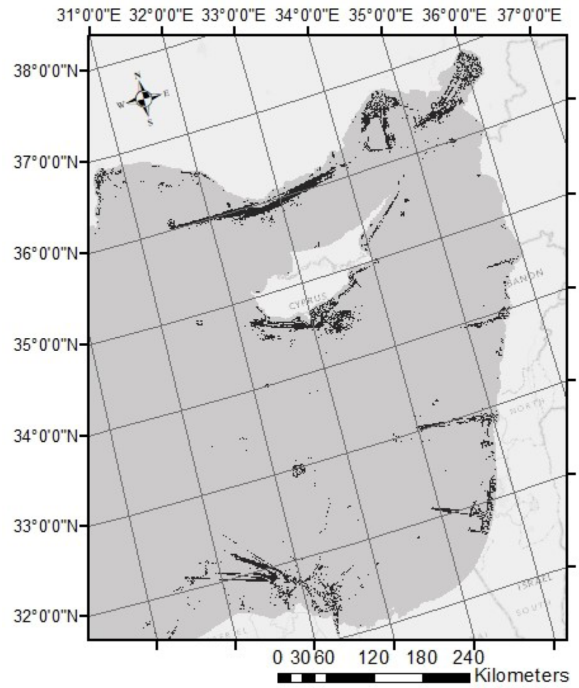

Figure 1. EMODnet projection for average vessel route and permanence density (2019). The darker regions indicate intense shipping activities.

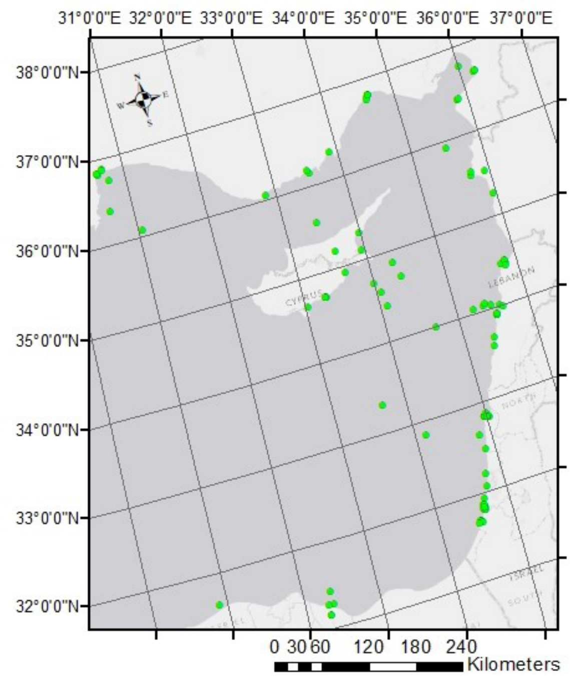

Figure 2. Accident occurrence spots provided by EMODnet in the Eastern Mediterranean Sea from 1977 to 2020. The solid circles in green colour were plotted on the map using ARCmap.

Alves *et al*. (2016) performed 19 simulations in the same region and found several oil-spill spots that beached in Cyprus. Three simulations showed a significant relative risk of oil invasion in Cyprus territory in which two spills were initiated between Cyprus island and Turkey, and one was initiated between Egypt and Cyprus. These simulations motived this paper to run an investigation taking the time range of one entire year with several spill points, in order to evaluate whether and from where the oil spill reaches the shoreline of Cyprus.

3. METHODOLOGY AND PRELIMINARY EXPECTATIONS

In order to address the relative potential impact, the developed methodology schematically represented in Figure 3. The platforms Mohid and Opendrift are used to include the pollutant trajectory dimension into such evaluation. In that sense, atmospheric and hydrodynamic information is required. Besides, in the construction of the relative risk indicator, a sensitivity scale to the impact assessment parameters was taken into account.

First, a simple relative impact risk assessment was run, based upon a formulation inspired by a common risk assessment concept used in engineering (Aven, 2012)also covering recent years. It is questioned if, and to what extent, it is possible to identify some underlying patterns in the way risk has been, and is being understood today. The analysis is based on a new categorisation of risk definitions and an assessment of these categories in relation to a set of critical issues, including how these risk definitions match typical daily-life phrases about risk. The paper presents a set of constructed development paths for the risk concept and concludes that over the last 1520 years we have seen a shift from rather narrow perspectives based on probabilities to ways of thinking which highlight events, consequences and uncertainties. However, some of the more narrow perspectives (like expected values and probability-based perspectives, which presents the interpretation for any impact I, considering the probability of this risk to happen P, and the consequences in case it happens C. Nevertheless, this paper adds two extra concepts: a barrier B and a constant α. The barrier would be the distance that the oil must travel to reach the shoreline, and is a sealing coefficient such that I lies in the range from 0% to 100%.

$$I = \frac{P \times C}{B} \times \alpha \qquad (1)$$

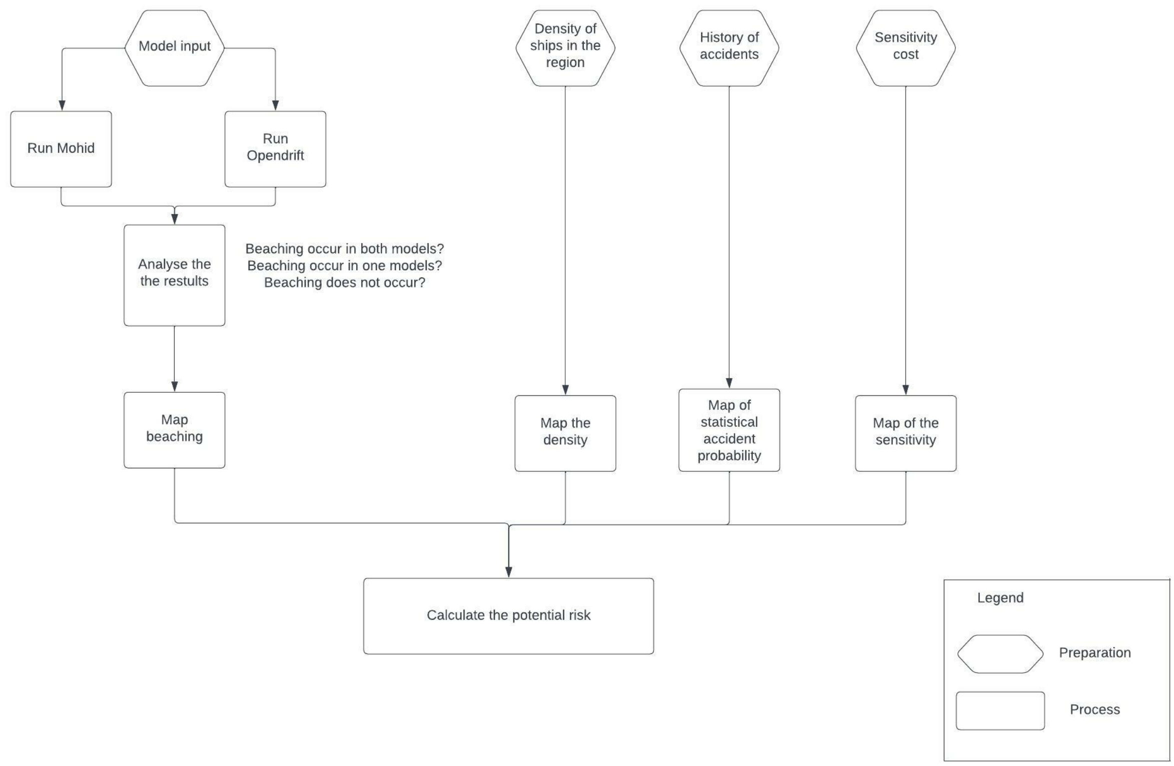

Figure 3. Schematic representation of the developed methodology.

In order to regulate the parameters to be used in this equation, it is considered that the probability of an accident to happen is intensified by the history of this location, whether and where the accidents have already happened; the occurrence and the density of the shipping activities in the region; and the period a vessel stays in the area, as it is expected that the longer it stays in the region, the higher is the risk of an accident. Oil spills in near regions can compromise the shoreline. A parametrisation was proposed for the calculation (see Table 1).

History parameter was taken from EMODNet history data for P; the distance D was retrieved by using ARCMap ruler measurement from the centre of each cell to the nearest corner snap of the island. The cost coefficient was designed to account for the difference each region can present when mitigation is required.

The study area was divided in a 6x6 fishnet projection in ARCmap, totalising in 36 cells, where four were excluded as they represent the land area (see Figure 4). Equation (1) was used to perform a preliminary heuristic classification for the oil spill event. The black mark indicates the georeferenced region. The areas were coloured following the relative impact risk results provided by Eq. (1). Some marks nearing the shoreline in the east were adjusted to be in the ocean area and they are not fitting the central coordinate accurately in the geometric forms.

Based on the results obtained: three distinct categories were created. Red category: in cases where the oil spill relative impact risk exceeded 60%. Yellow category: in cases between 10% and 60%. Gray category: low significance - for cases until 10% (see Figure 4).

The first observation reinforces, as expected, that areas nearing the country are more sensitive to oil spill events. The four red cells, located in the north and the south of the country, implies in a considerable risk of oil spill impact. The consequences could reach a wide length of Cyprus' shoreline.

Table 1. Parameters proposed to use in Eq(1).

Variables	**Input**	**Definition**	**Unit**
P	1-5	1 = no history reported or one accident reported	Dimensionless variable
		2 = two reported accidents in the region	
		3 = three reported accidents in the region	
		4 = four reported accidents in the region	
		5 = more than five reported accidents	
C	0-20	Estimated cost coefficient of the shoreline affected	Dimensionless variable
B	50-450	Distance from Cyprus' shoreline	Km
α	0.5	Fixed Correction Value	km^{-1}

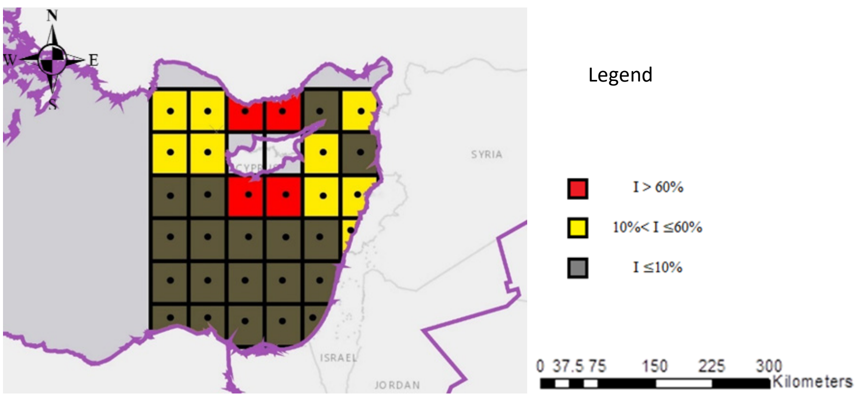

Figure 4. Eastern Mediterranean Sea grid cells and preliminary heuristic impact risk classification, Eq.(1). Grey: I≤10%; Yellow: 10%<I≤60%; Red: I >60%.

The eastern regions of Cyprus presented two different interlaying categories, represented by yellow and grey cells. This situation happened due to the accidents recorded in the region rather than to the vessel density. In the west region of Cyprus, the northern sea oil spills yield a moderate impact risk, and the main reason is the proximity to the country.

The south region of the Cypriot sea was uniform with respect to the preliminary heuristic relative impact assessment. Induced by the distance, the relative impact risk assessment reached significantly low results, even with occasional accidents, that would result in a 7.5% risk. The port regions of Cyprus neighbouring countries have a high density of vessels and a prolonged stay, which contributed to the moderate estimated impact risk. The distance, nevertheless, is expected to reduce the risk for Cyprus, significantly.

Model Implementation

In this work, it is used the Copernicus catalogue for maritime data. In Copernicus, the database for this region can be found for every single hour in MEDSEA_ANALYSIS_FORECAST_PHY_006_013 dataset (Clementi *et al.*, 2019) as well as the bathymetry, which is found on the dataset GLOBAL_ANALYSIS_FORECAST_WAV_001_027 (Ardhuin *et al.*, 2010). Atmospheric data was incorporated from the NOAA/NCEP catalogue NCEP GFS 0.25 Degree Global Forecast Grids Historical Archive - 6-hour timeframe (NCEP, 2015). A non-specific type of oil was used in the simulations presented in this work, with attention to the oil properties that are compatible with the tankers' content in the region of interest.

A 10-day simulation was deliberately chosen as it is expected that after this period, emergency actions would have already been carried out and the simulation would lose its reliability.

The periods were decided to take into consideration the different moon phases and extreme temperatures in all months of the year 2020 (see Tables 2 and 3).

All the simulations were performed on the same group of coordinates and using the same properties. The projection in Figure 4 was used as a starting point. The projection returned 36 coordinates from which four coordinates were discarded as they occurred in regions of land. Thus, a total of 32 coordinates per month were computed and simulated individually, totalising 384 simulations (32 simulations x 12 months).

4. RESULTS AND DISCUSSION

Both platforms used in this work - Mohid and Opendrift - are programmed to trace the oil considering the physical and chemical properties and its fate. Mohid and Opendrift achieve the oil fate by spreading, advection, and diffusing of the oil particles, which is incorporated in a Lagrangian module so as to compute the spatial evolution of these particles according to the calculated or imposed wind drift values, ocean current velocity, particle movement, and a random velocity (diffusive transport) (Fernandes, 2017; Rodrigues, 2012). The difference between the platforms is the equations that rule over the calculations.

The random walk and Stokes drift, for instance, are retrieved by different mathematical formulations in Mohid and Opendrift. For random walk in Mohid, the initial velocity (u') is reduced as the tracers pass through the mixing length (L). The adapted method from Allen (1982) and Sullivan (1971) proposes the random movement. The time to have a random walk is the mixing length divided by the standard deviation of the turbulent velocity $dt = \frac{L}{\sqrt{\overline{u'u'}}}$. Provided that the mass flux (x) is dependent on the water turbulence to move and

Table 2. Pre-defined timeseries for the first semester of 2020.

Months:	**1**	**2**	**3**	**4**	**5**	**6**
Days	3/Jan-13/Jan	25/Feb-5/Mar	24/Mar-3/Apr	15/Apr- 25/Apr	7/May-17/May	13/Jun-23/Jun
Period:	¼ moon	Lowest water °C	New moon	¾ moon	Full moon	¼ moon

Table 3. Pre-defined timeseries for the second semester of 2020.

Months:	**7**	**8**	**9**	**10**	**11**	**12**
Days	05/Jul-15/Jul	05/Aug-15/Aug	17/Sep-27/Sep	10/Oct- 20/Oct	30/Nov-10/Dec	14/Dec-24/Dec
Period:	¾ moon	Highest water °C	New moon	¾ moon	¾ moon	New moon

considering that traceable particles are emitted in a specific spot x=0, it means that $\frac{d}{dt}(\overline{x^2}) = 2\overline{xu'}$. As the correlation between x and u' is extremely low $\overline{xu'} \to 0$ when $x>L$, a modification of language is proposed and $\overline{xu'} = u_t L$, where $u_t = \sqrt{\overline{u'u'}}$, indicating the square root of the variance of the turbulent velocity in the function of x and the mixing length L. When the velocity is thoroughly through, it is restarted based on a statistical distribution of null average and variance (u_t^2). L values can be constant or not depending on the means it flows through. The values admitted by the platform consider L and u_t as a constant value throughout the complete domain, as demonstrated in Table 4.

For random walk in Opendrift, Visser (1997) observed after experimentations that tracers at a particular position (depth) are influenced by eddies with different energy levels, making them not constant. This observation proposes a method that is not related to stochastic differential equations. Rather, it proposes that diffusivity K(m²s⁻¹) of the square of the particle movement z in a 1-dimensional situation is $\frac{d}{dt}(Z^2) = 2k$. As position changes Z_n to Z_n+1 along the time δt, the work presented $Z_{n+1} = Z_n + R(2r^{-1}K\delta t)^{1/2}$, considering R the random process, mean and standard deviation respectively $(R^2) = 0$ and $(R^2) = r$. Finally, the boundary conditions are implemented in the model giving the equation in Table 4.

Particles are also induced by waves (Stokes drift) and the platforms differ in their mathematical approach. For Mohid, the stokes transport (u_s) for all particles is calculated individually and added up to its horizontal velocity component (see Table 4) (Daniel *et al.*, 2003). The depth has a major influence over the stokes drift effect so a depth independent term (C) is proposed as an arbitrary constant $C = \frac{-a^2\sigma \; sinh\; 2kh}{4h\; sinh^2\; kh}$, where a = wave amplitude, $k = 2\pi/L$ whereas L = wavelength, h = depth, and $\sigma = 2\pi/P$, whereas P = wave period (Longuet-Higgins, 1953) apart from their orbital motion, a steady second-order drift velocity (usually called the mass-transport velocity.

In Opendrift the Stokes drift velocity profile is based on Phillips spectrum, which gives a fair approximation based on the equilibrium range of the spectrum of waves forced by the wind above the spectral peak (Breivik *et al.*, 2013) see Table 4. The Stoken transport in Opendrift depends on the Phillips spectrum profile, which is expected to balance the equation of the spectrum of waves forced by the wind above the spectral peak. A coefficient β for the Phillips spectrum is presented in Breivik *et al.*(2013) work and commonly retrieves exactly one. However, an approximated formulation is also presented as: $\hat{\beta} = \frac{2(w^5 F(w))}{g v_0 w_p}$ in a one-dimension frequency spectrum , where w = circular frequency, $F(w)$ = Frequency spectrum, g = gravity, v_0 = initial stokes drift velocity, wp = peak frequency (Breivik *et al.*, 2016; Janssen, 2009).

Table 4. Random walk and Stokes drift methods in software compilation.

Phenomenon	Platform	Random walk behaviour	Reference
Random walk	Mohid	$dt = \frac{L}{u_t}$	(Allen, 1982; Sullivan, 1971)551–576 (1971
	Opendrift	$z_{n+1} = z_n + K'(z_n)\delta t + R\left\{2r^{-1}K\left[z_n + \frac{1}{2}K'(z_n)\delta t\right]\delta t\right\}^{\frac{1}{2}}$	Visser (1997)
Stokes drift	Mohid	$u_s = a^2 \cdot w \cdot k\frac{cosh[2 \cdot k(z-h)]}{2 \cdot sinh^2(k \cdot h)} + C$	Daniel *et al.* (2003) and Longuet-Higgins (1953)
	Opendrift	$V = \frac{V0}{2k_p}(1 - \frac{2\beta}{3})$	Breivik *et al.*, (2016)

Where in Mohid equation (random walk): dt = time variation, L = mixing length, and $\sqrt{\overline{u'u'}}$. In Opendrift equation (random walk): z = particle displacement, K' = diffusivity derivate, δt= time delta, R = random process. In Mohid equation (Stokes drift): z = depth underneath surface, a = wave amplitude, w = wave circular frequency, k = wave number, C = depth independent term. And in Opendrift: V = Stokes drift velocity, V0=surface velocity, kp = peak wavenumber, β = constant.

Figure 5 shows the steps considered in the methodology application indicating, also, the corresponding figures with the input information and results obtained.

The simulation provided results for each month and as can be seen for the first semester predictions (Figure 6) and the second semester predictions (Figure 7). The results suggested that 11 out of the 32 simulated points of oil discharge led to a beaching effect, and all of them near Cyprus.

In simulations made for the October and November months, the first row of cells (to the south closer to the Cyprus shoreline) presented a beaching effect. Nevertheless, the next rows to the south did not have the same result in any period within the 12 months of simulations. Qiao *et al*. (2019) made 19 simulations over the same region and created several spill origins based in port regions or nearby, mainly in the Egypt and Israel shore regions. The result suggested that five emissions reached the Cypriot shore, two from the northern region and the other three from the south. The variations observed between this work and others seem to be reasonable as the timeframe chosen for simulations are not expected to be the same and many phenomena change their behaviour throughout the years. An additional plausible reason would be the anticyclonic eddies located in the south region of Cyprus, i.e. the Shikmona gyre (Zodiatis *et al*., 2005). The simulations with Mohid showed a higher dispersity of the oil particles in the first moments of the simulations, whilst Opendrift showed a neat round movement of several oil slicks in the same region and at the same period. Shikmona gyre phenomenon could have modified the trajectory of the particles in a different direction other than toward Cyprus.

The results from both platforms indicate that in February, no oil spill from any area would reach the Cypriot shoreline. It was a unique condition that hindered the proximity of the oil slick

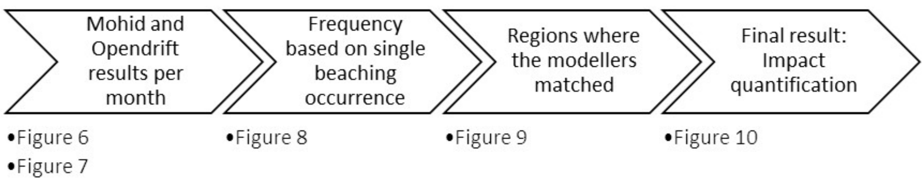

Figure 5. Methodology steps and results presentation structure.

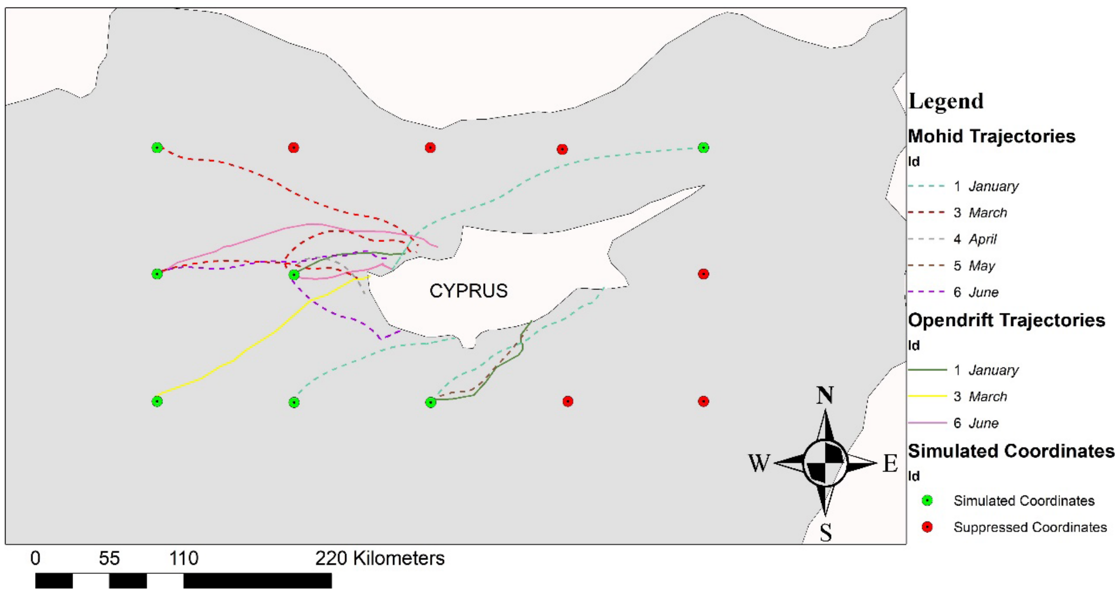

Figure 6. Simulations for the first semester of 2020 in Mohid and Opendrift.

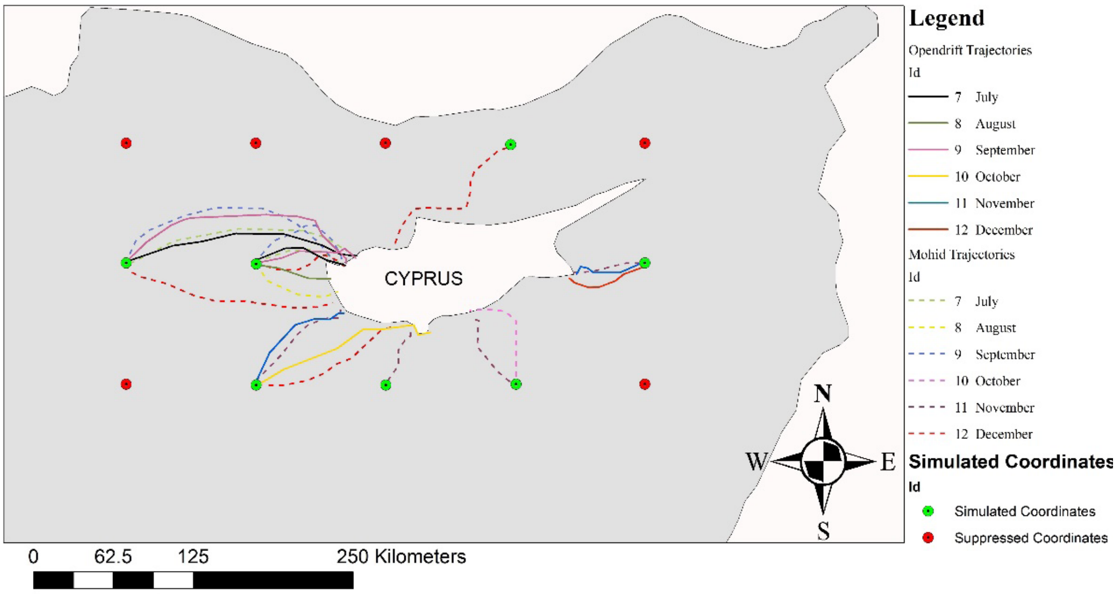

Figure 7. Simulations for the second semester of 2020 with both Mohid and Opendrift platforms.

throughout its trajectory. The movement of the oil slick from the north-eastern region of the sea revealed moments that the northern coast in the island was hit by the oil, after a while, a northward trend onto Turkey country was perceived and the oil no longer threatened the island. Particles did not present a strong dispersion, which may be due to two reasonable reasons: (1) Hydrodynamic effect caused by the coldest temperature or (2) Coincident non-favourable hydrodynamic/weather in the period selected. The latter could explain the phenomenon that made November simulations remarkable for their rapidness and intensity in a westward movement in the East of Cyprus (in the Famagusta region).

Further, all the months except for February, October, and November had oil spills that reached the Cypriot shoreline sourcing from the west region of the sea. It is clear at this stage that the west of Cyprus is a critical area to be considered in oil spill events.

Simulations with both Mohid and Opendrift for June and July months, had the same oil spill origins being responsible for the beaching effect, indicating a lengthy period of an eastward trend that affected Cyprus intensively.

An interesting overall observation of the simulations demonstrated that both platforms could often show equivalent results. From the oil spill locations, Mohid resulted in more beaching results (24) compared to Opendrift (18) in the entire period of simulations. Mohid and Opendrift presented a perfect match for the oil spill location and the corresponding results in eleven simulations (see Figures 6 and 7). Months that did not have the beaching effect were not included in the figures.

One thought-provoking observation for December simulations is that Opendrift presented one individual location for the beached oil source (east - near Famagusta region), whilst Mohid showed four distinct spots: three in the west and one in the north of the country. The simulations for December showed the largest discrepancy in the computational platforms' outputs compared to the other simulations.

In sequence, it was observed the importance of coupling both estimations by an evaluation relating the frequency of beaching occurrences and the corresponding oil spill locations. The results created Figure 8 and summarises the 42 beached spills (24 – Mohid and 18 – Opendrift). The red cells represent particularly important locations, since there is a high frequency of occurrences (from nine to twelve), the yellow marks represent a moderate range from six to eight occurrences, and the grey cells indicate low frequency from one to five occurrences. Observe that this colour scale is not related to the one used to indicate the preliminary heuristic impact risk classification graphically shown in Figure 4, with the calculated values obtained with Eq.(1).

In Figure 9, it is possible to observe the agreement between both platforms, Mohid and Opendrift. The red cells indicate the highest frequency of occurrences (three matches). In the yellow cell, it reached two simulations. The grey cells present locations that the platforms matched only once.

The region on the west of Cyprus showed high significance in this impact risk assessment, implying that an oil spill in the west region would have a higher risk of reaching the shoreline.

All the simulations were performed in an Intel ® Core (TM) i7-8565U CPU @ 1.8 GHz with 8GB RAM in Windows 10 Professional OS. The simulation processing time for each month in Mohid was about 2 hours while in Opendrift, about 20 minutes.

5. RELATIVE POTENTIAL IMPACT ASSESSMENT

In order to decide which areas are more sensible regarding oil spills and corresponding beaching occurrence, a simplified empirical relative potential impact assessment was proposed based on the preliminary heuristic evaluation given by Eq.(1), incorporating new effects, supported by the platforms Mohid and Opendrift.

$$R_q = \beta \cdot \left(\frac{R_{cell} \times S \times M \times C_1 \times d \times H}{D}\right) \qquad (2)$$

The parameters used to calculate R_q are described in Table 5.

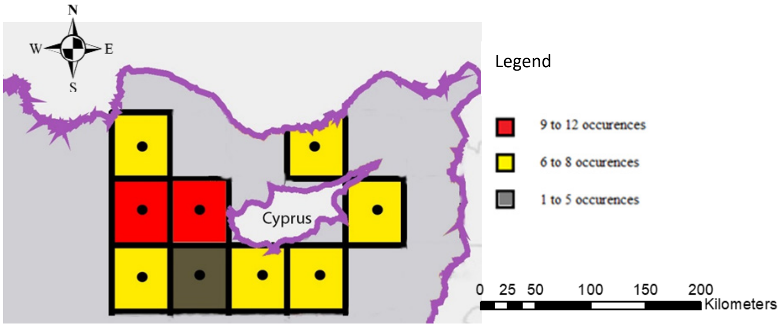

Figure 8. Frequency based on single beaching occurrence where grey: 1 to 5; 6≤yellow≤8; 9≤red≤12 occurrences.

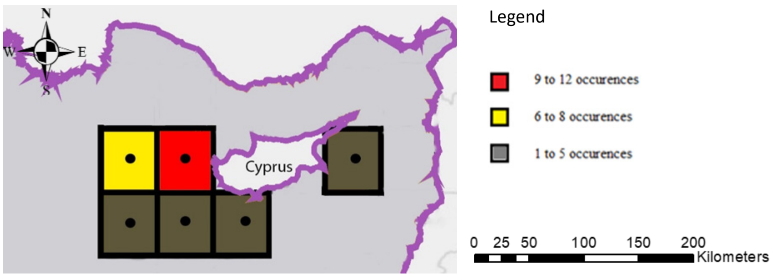

Figure 9. Regions where the Mohid and Opendrift beaching results matched. Red: 3 matches; Yellow: 2 matches; Grey: 1 match.

Table 5. Parameters proposed to use in Eq (2) for the relative potential impact assessment Rq.

Description	Values	Unit	Meaning
Risk cell, ***Rcell***	1, 25, 50	Dimensionless	Increasing values according to the cell High-risk cells (50), moderate risk cells (25), lower risk cells (1)
Sensitivity, ***S***	1 or 5	Dimensionless	If it is a classified region (5); otherwise (1)
Matches, ***M***	1 or 5	Dimensionless	If both programmes match the region (5); otherwise (1)
Hit the Target, C_1	0 or 1	Dimensionless	If models hit the target (1); otherwise (0)
Vessel Density, ***d***	1 or 2	Dimensionless	For high density (2); For low density (1)
History, ***H***	1 or 2	Dimensionless	Prior accident reported in the block (2); No prior accident reported (1)
Distance, ***D***	Distance value >50	km	For distances < 50km use D = 5.0km
Constant, β	0.25	km^{-1}	Fixed value

Some particularities must be considered in order to have appropriate use of Eq.(2). This paper understands that the frequency of accidents (H) reported (Figure 2) is relevant to estimate the risk of a new accident occurrence. There are many known reasons which can develop into an accident such as human mistakes, machinery problems, and weather conditions. Even a single vessel could have problems with the machinery or anchoring procedures which would lead to spillage. It is expected that intense vessel density (Figure 1) would strengthen the risk of an accident (d), however, the distance (D) to the shoreline is expected to be an obstacle for the spilled oil to reach the land.

Based on the simulation outputs (Figure 8 and Figure 9), a risk cell argument ($Rcell$) and a confirmation based on equivalent outputs (M) were created in the equation, so that it is possible to qualify a relevant risk of a beaching effect. A beaching effect is always an unwanted effect that can happen after a spillage; however, environmental problems are relevant even though the oil does not reach the shore. This paper did not study the sensitivity of the regions thoroughly (S). Rather, it is based on the premise that the south of the island is the most sensitive area. This premise is because aquaculture and tourism hotspots are present in this region (Cyprus, 2021, 2019). The simulation platforms were quite significant (Fig 9) at this stage, presenting whether the oil would reach the shoreline (C_1). In order to provide a reasonable scale of the relative potential impact assessment, a constant β was created.

Based on Eq. (2), Figure 11 was created. Three distinct categories were created and represented in Figure 11 with a colour scale. Red indicates R_q > 50, yellow: 2.5% < R_q ≤ 50%, and grey: R_q ≤ 2.5%.

Different volumes of oil spills over the Eastern Mediterranean Sea could result in a different dispersion in the model. For instance, it is expected that in case of a large oil spill in the south of the region (near the Israel coastline), some particles could eventually reach the Cypriot country due to the atmosphere and hydrodynamic forces. These regions have intense shipping activities and a history of accidents, increasing the beaching risk. The numerically low relative risk areas (in grey) corroborate what has been discussed in this work.

The red areas, however, still represents a threat to the country in nearby areas. Equations (1) and (2) provided different results, as can be observed in Figures 4 and 10 as more details were inserted in the calculation of R_q. In only one situation they matched the location (red cell in the south of Cyprus shoreline), reinforcing the importance of this area in the dynamics of an oil spill event.

6. SENSIBLE REGIONS IN CYPRUS

The simulations performed in this work indicated a strong movement of oil particles toward Limassol (south), Paphos (west), and Paralimni (east). According to tourism statistics provided by the Ministry of Finance from Cyprus, these three regions correspond to 63% of all tourism in Cyprus (35.5% Paphos; 14% Paralimni; and 13.6% in Limassol) (Cyprus, 2019).

Aquaculture economy is also present in Cyprus and the data provided by the Department of Fisheries and Marine Research of Cyprus acknowledges that pandora (*Pagellus erythrinus*), gilthead seabream (Sparus aurata), red bream (*Pagrus pagrus*), Japanese bream (*Pagrus major*), and meagre (*Argyros omusregius*), European seabass (*Dicentrachus labrax*), rabbitfish (*Siganus rivulatus*), and shrimps are present in aquaculture activities which are located closer to the shore (Cyprus, 2021).

When there is an oil spill, the insoluble fraction remains in surface forming a layer that blocks gas exchange and light permeation in the water column (Gomes *et al*., 2017) affecting the photosynthesis process (Newman and Clements, 2008). The soluble part, such as benzene, toluene, and xylene (Baird and Cann, 2012; Doherty *et al*., 2019; Niaz *et al*., 2015), although highly diluted in the ocean, are polycyclic hydrocarbons that bind to the biotic ligand. After its metabolization, the organisms develop highly reactive metabolites, which are extremely toxic, affecting the organism's life severely by disorders in metabolism, oxidative stress, genotoxicity, morphological damage, and endocrine disruption (Gomes *et al*., 2017; Newman, 2015). Humans can also be affected by consuming these organisms (EFSA, 2012; Osuagwu and Olaifa, 2018).

It is still not possible to predict all consequences the oily water may result (Grosell and Pasparakis, 2021; Pasparakis *et al*., 2019; Ward, 2017). It is common knowledge that physical and chemical modification in the water will alter the equilibrium framework of the region jeopardising the survival and the reproduction of these organisms (Chen *et al*., 2019; Gomes *et al*., 2017).

7. CONCLUSIONS

The current and yet growing demand for petroleum encourages researchers to find means to mitigate the negative consequences of this activity.

The use of computational platforms based on mathematical modelling proved to be essential to predict critical areas in case of an oil spill. Due to computational limitations, it was reasonable to propose a heuristic preliminary expectation and limit the simulation area. In addition, using two different platforms providing equivalent results reinforced the results, mainly because they are based on different mathematical backgrounds.

Based on a relative potential impact assessment equation, the simulations suggested that accidents happening near Cyprus are far more critical. Regions such as Paphos, Limassol, and Paralimni had the most critical classification. These regions are Cypriot economy hotspots for tourism and aquaculture and their protection is highly recommended. However, the region is a path where several ships travel during the year and the possibility of an accident and a beaching effect is considerable.

It was interesting to use both platforms to compare the oil spill results. They could provide clear and precise predicted information regarding the trajectory performed by the oil. Besides that, the equivalence of the results was valuable to this work suggesting that even different mathematical models for some spillages in specific coordinates would reach the same results. Both platforms are open-source code, which is an advantage for researchers.

Identifying potential risks and consequences in case of an oil spill is an important strategy to certify the wellness and emergency actions in case of necessity. Computational models are important tools that allow systematic approaches which are helpful to enhance the assessment of an oil spill event and the design of remediation measures, besides increasing the readiness for the realisation of such measures.

Future research could examine the sensitivity of the region of Cyprus, providing more precise sensitivity argument, mainly in aquaculture regions, considering the biological disturbances in case of an oil spill event.

AUTHOR CONTRIBUTION

Several approaches regarding oil spills are found on scientific literature, nevertheless, the research to produce this paper could not find any metric or explanation over the procedure decision. This paper aims to provide a procedure to evaluate the relative potential impact throughout the countries shorelines and is expected to be a complementary tool for decision making processes.

ACKNOWLEDGEMENT

The authors acknowledge the financial support provided by FAPERJ, Fundação Carlos Chagas Filho de Amparo à Pesquisa do Estado do Rio de Janeiro, CNPq, Conselho Nacional de Desenvolvimento Científico e Tecnológico and CAPES, Coordenação de Aperfeiçoamento de Pessoal de Nível Superior (Finance Code 001).

REFERENCES

Al-Rabeh, A.H., Cekirge, H.M., Gunay, N., 1989. A stochastic simulation model of oil spill fate and transport. *Applied Mathematical Modelling* 13, 322–329. https://doi.org/10.1016/0307-904X(89)90134-0

Allen, C.M., 1982. Numerical simulation of contaminant dispersion in estuary flows. Proceedings of the Royal Society of London. A. *Mathematical and Physical Sciences* 381, 179–194. https://doi.org/10.1098/rspa.1982.0064

Alves, T.M., Kokinou, E., Zodiatis, G., Radhakrishnan, H., Panagiotakis, C., Lardner, R., 2016. Multidisciplinary oil spill modeling to protect coastal communities and the environment of the Eastern Mediterranean Sea. *Scientific Reports* 6, 36882. https://doi.org/10.1038/srep36882

Ardhuin, F., Rogers, E., Babanin, A. V., Filipot, J.F., Magne, R., Roland, A., van der Westhuysen, A., Queffeulou, P., Lefevre, J.M., Aouf, L., Collard, F., 2010. Semiempirical dissipation source functions for ocean waves. Part I: Definition, calibration, and validation. *Journal of Physical Oceanography* 40, 1917–1941. https://doi.org/10.1175/2010JPO4324.1

Aven, T., 2012. The risk concept-historical and recent development trends. *Reliability Engineering and System Safety* 99, 33–44. https://doi.org/10.1016/j.ress.2011.11.006

Baird, C., Cann, M.C., 2012. Environmental chemistry, 5th ed. ed. W.H. Freeman, New York.

Balogun, A.-L., Yekeen, S.T., Pradhan, B., Wan Yusof, K.B., 2021. Oil spill trajectory modelling and environmental vulnerability mapping using GNOME model and GIS. Environmental Pollution 268, 115812. https://doi.org/10.1016/j.envpol.2020.115812

Breivik, Ø., Bidlot, J.-R., Janssen, P.A.E.M., 2016. A Stokes drift approximation based on the Phillips spectrum. Ocean Modelling 100, 49–56. https://doi.org/10.1016/j.ocemod.2016.01.005

Breivik, Ø., Janssen, P.A.E.M., Bidlot, J.-R., 2013. 716 Approximate Stokes Drift Profiles in Deep Water.

Chen, H., Li, D., Li, X., 2007. Mathematical Modeling of Oil Spill on the Sea and Application of the Modeling in Daya Bay. Journal of Hydrodynamics 19, 282–291. https://doi.org/10.1016/S1001-6058(07)60060-2

Chen, J., Zhang, W., Wan, Z., Li, S., Huang, T., Fei, Y., 2019. Oil spills from global tankers: Status review and future governance. Journal of Cleaner Production 227, 20–32. https://doi.org/10.1016/j.jclepro.2019.04.020

Clementi, E., Pistoia, J., Escudier, R., Delrosso, D., Drudi, M., Grandi, A., Lecci, R., Cretì, S., Ciliberti, S.A., Coppini, G., 2019. Mediterranean Sea Analysis and Forecast (CMEMS MED-Currents 2016-2019).

Cyprus, 2021. DEPARTMENT OF FISHERIES AND MARINE RESEARCH - Aquaculture. In: http://www.moa.gov.cy/moa/dfmr/dfmr.nsf/All/C543D53DAC6EE96C42257EA0003430C9?OpenDocument (accessed 3.18.21).

Cyprus, 2019. MOVEMENT OF TRAVELLERS, 1980-2019 [WWW Document]. In: https://www.mof.gov.cy/mof/cystat/statistics.nsf/All/802B288B5F25DDB3C225779E00314F02/$file/TOURISM_STATISTICS-JANDEC19-EN-140820.xls?OpenElement (accessed 10.31.20).

Dagestad, K.-F., Breivik, Ø., \rAdlandsvik, B., 2016. OpenDrift - an open source framework for ocean trajectory modeling, in: EGU General Assembly Conference Abstracts, EGU General Assembly Conference Abstracts. pp. EPSC2016-7282.

Dagestad, K.-F., Röhrs, J., Breivik, Ø., Ådlandsvik, B., 2018. OpenDrift v1.0: a generic framework for trajectory modelling. Geoscientific Model Development 11, 1405–1420. https://doi.org/10.5194/gmd-11-1405-2018

Daniel, P., Marty, F., Josse, P., Skandrani, C., Benshila, R., 2003. Improvement of Drift Calculation in Mothy Operational Oil Spill Prediction System. International Oil Spill Conference Proceedings 2003, 1067–1072. https://doi.org/10.7901/2169-3358-2003-1-1067.

Doherty, F. V, Aneyo, I., Otitoloju, A.A., 2019. Histopathological and biochemical alterations in Eudrilus eugeniae (Kinberg 1867) as biomarkers of exposure to monocyclic aromatic hydrocarbons in oil impacted site. The Journal of Basic and Applied Zoology 80, 63. https://doi.org/10.1186/s41936-019-0130-2

EFSA, 2012. Scientific Opinion on Mineral Oil Hydrocarbons in Food, EFSA Journal. Wiley-Blackwell Publishing Ltd. https://doi.org/10.2903/j.efsa.2012.2704

El-Geziry, T.M., Bryden, I.G., 2010. The circulation pattern in the Mediterranean Sea: issues for modeller consideration. Journal of Operational Oceanography 3, 39–46. https://doi.org/10.1080/1755876X.2010.11020116

EMSA, 2019. EMODnet Human Activities: EMSA Route Density Map. In: https://www.emodnet-humanactivities.eu/search-results.php?dataname=Route+density+%28source%3A+EMSA%29 (accessed 1.1.21).

Fernandes, R., 2017. Bibliographic review of HNS spill model (MOHID). In: http://wikimariner.actionmodulers.com/wiki/images/7/72/HNS_model_bibliographic_review_-_scientific_manual.pdf (accessed 12.22.20).

Gomes, A.R.C., Delunardo, F.A.C., Sadauskas-Henrique, H., Braz Mota, S., de Almeida-Val, V.M.F., 2017. Chapter 12. Genotoxic and Biochemical Responses Triggered by Polycyclic Aromatic Hydrocarbons in Freshwater and Marine Fish: Tambaqui and Seahorse as Bioindicators. pp. 278–304. https://doi.org/10.1039/9781782629887-00278

Grosell, M., Pasparakis, C., 2021. Physiological Responses of Fish to Oil Spills. Annual Review of Marine Science 13, annurev--marine--040120--094802. https://doi.org/10.1146/annurev-marine-040120-094802

Ha, M.J., 2018. Modeling for the allocation of oil spill recovery capacity considering environmental and economic factors. Marine Pollution Bulletin 126, 184–190. https://doi.org/10.1016/j.marpolbul.2017.11.006

ITOPF, 2020. Oil tanker spill statistics. In: https://www.itopf.org/fileadmin/data/Documents/Company_Lit/Oil_Spill_Stats_brochure_2020_for_web.pdf (accessed 1.8.20).

Janssen, P., 2009. The energy balance of deep-water ocean waves, in: The Interaction of Ocean Waves and Wind. Cambridge University Press, pp. 7–55. https://doi.org/10.1017/cbo9780511525018.003

Johns, L., 2019. EMODnet Human Activities: Vessel Density Map. In: https://www.emodnet-humanactivities.eu/ (accessed 1.1.21).

Jones, C.E., Dagestad, K.-F., Breivik, Ø., Holt, B., Röhrs, J., Christensen, K.H., Espeseth, M., Brekke, C., Skrunes, S., 2016. Measurement and modeling of oil slick transport. Journal of Geophysical Research: Oceans 121, 7759–7775. https://doi.org/10.1002/2016JC012113

Katircioglu, S., 2009. Tourism, trade and growth: The case of Cyprus. Applied Economics 41, 2741–2750. https://doi.org/10.1080/00036840701335512

Kirkos, G., Zodiatis, G., Loizides, L., Ioannou, M., 2018. Oil pollution in the waters of Cyprus, in: Handbook of Environmental Chemistry. pp. 229–245. https://doi.org/10.1007/698_2017_49

Kostianoy, A.G., Carpenter, A., 2018. History, sources and volumes of oil pollution in the mediterranean sea. Handbook of Environmental Chemistry 83, 9–31. https://doi.org/10.1007/698_2018_369

Lemesios, G., Giannakopoulos, C., Papadaskalopoulou, C., Karali, A., Varotsos, K. V, Moustakas, K., Malamis, D., Zachariou-Dodou, M., Petrakis, M., Loizidou, M., 2016. Future heat-related climate change impacts on tourism industry in Cyprus. Regional Environmental Change 16, 1915–1927. https://doi.org/10.1007/s10113-016-0997-0

Li, P., Niu, H., Li, S., Fernandes, R., Neves, R., 2017. A Comprehensive System for Simulating Oil Spill Trajectory and Behaviour in Subsurface and Surface Water Environments. International Oil Spill Conference Proceedings 2017, 1251–1266. https://doi.org/10.7901/2169-3358-2017.1.1251

Ličer, M., Estival, S., Reyes-Suarez, C., Deponte, D., Fettich, A., 2020. Lagrangian Trajectory Modelling for a Person lost at Sea during Adriatic Scirocco Storm of 29 October 2018. Natural Hazards and Earth System Sciences 1–19. https://doi.org/10.5194/nhess-2019-362

Longuet-Higgins, M.S., 1953. Mass transport in water waves. Philosophical Transactions of the Royal Society of London. Series A, Mathematical and Physical Sciences 245, 535–581. https://doi.org/10.1098/rsta.1953.0006

Lugon Jr., J., Juliano, M.M., Kyriakides, I., Yamasaki, E.N., Rodrigues, P.P.G.W., Silva Neto, A.J., 2020. Environmental hydrodynamic modelling applied to extreme events in Caribbean and Mediterranean countries. DESALINATION AND WATER TREATMENT 194, 315–323. https://doi.org/10.5004/dwt.2020.25819

Mavris, C., 2011. Sustainable Environmental Tourism and Insular Coastal Area Risk Management in Cyprus and the Mediterranean. Journal of Coastal Research 61, 317–327. https://doi.org/10.2112/SI61-001.32

Millot, C., Taupier-Letage, I., 2005. Circulation in the Mediterranean Sea, in: Handbook of Environmental Chemistry. pp. 29–66. https://doi.org/10.1007/b107143

Miranda, R., Braunschweig, F., Leitão, P., Neves, R., Martins, F., Santos, A., 2000. MOHID 2000 - A coastal integrated object oriented model, Water Studies. WIT Press. https://doi.org/10.2495/HY000371

NCEP - National Centers for Environmental Prediction/National Weather Service/NOAA/U.S, 2015. NCEP GFS 0.25 Degree Global Forecast Grids Historical Archive. In: https://doi.org/https://doi.org/10.5065/d65d8pwk

Neves, R., 1985. Bidimensional model for residual circulation in coastal zones: application to the Sado estuary. Annales geophysicae 3, 465–471.

Newman, M.C., 2015. Fundamentals of Ecotoxicology - The Science of Pollution, CRC Press/Taylor & Francis.

Newman, M.C., Clements, W.H., 2008. Ecotoxicology: a comprehensive treatment. CRC Press, Boca Raton, FL.

Niaz, K., Bahadar, H., Maqbool, F., Abdollahi, M., 2015. A review of environmental and occupational exposure to xylene and its health concerns. EXCLI Journal; 14:Doc1167; ISSN 1611-2156. https://doi.org/10.17179/EXCLI2015-623

Nikolaidis, A., Akylas, E., Michailides, C., Moutsiou, T., Leventis, G., Constantinides, A., McCartney, C., Demesticha, S., Kassianidou, V., Zomeni, Z., Bar-Yosef Mayer, D., Makovsky, Y., Kyriakidis, P., 2020. Modeling drift-induced maritime connectivity between Cyprus and its surrounding coastal areas during early Holocene, in: EGU General Assembly Conference Abstracts, EGU General Assembly Conference Abstracts. p. 19782.

Oliveira, A.R., Ramos, T.B., Simionesei, L., Pinto, L., Neves, R., 2020. Sensitivity Analysis of the MOHID-Land Hydrological Model: A Case Study of the Ulla River Basin. Water 12, 3258. https://doi.org/10.3390/w12113258

Osuagwu, E.S., Olaifa, E., 2018. Effects of oil spills on fish production in the Niger Delta. PLOS ONE 13, e0205114. https://doi.org/10.1371/journal.pone.0205114

Paiva, P.M., Lugon Junior, J., Barreto, A.N., Silva, J.A.F., Silva Neto, A.J., 2017. Comparing 3d and 2d computational modeling of an oil well blowout using MOHID platform - A case study in the Campos Basin. Science of The Total Environment 595, 633–641. https://doi.org/10.1016/j.scitotenv.2017.04.007

Pasparakis, C., Esbaugh, A.J., Burggren, W., Grosell, M., 2019. Impacts of deepwater horizon oil on fish. Comparative Biochemistry and Physiology Part - C: Toxicology and Pharmacology. https://doi.org/10.1016/j.cbpc.2019.06.002

Qiao, F., Wang, G., Yin, L., Zeng, K., Zhang, Y., Zhang, M., Xiao, B., Jiang, S., Chen, H., Chen, G., 2019. Modelling oil trajectories and potentially contaminated areas from the Sanchi oil spill. Science of the Total Environment 685, 856–866. https://doi.org/10.1016/j.scitotenv.2019.06.255

Rodrigues, P.P.G.W., 2012. MOHID Description / MARETEC, 1st ed. Essentia Editora, Campos dos Goytacazes, RJ, Brazil.

Silva, A., de Pablo, H., Moita, M.T., Quental, T., Pinto, L., 2013. Ocean modelling for coastal management – Case studies with MOHID using Lagrangian elements to simulate alongshore transport of harmful algal blooms. IST Press.

Sullivan, P.J., 1971. Longitudinal dispersion within a two-dimensional turbulent shear flow. Journal of Fluid Mechanics 49, 551. https://doi.org/10.1017/S0022112071002258

Visser, A.W., 1997. Using random walk models to simulate the vertical distribution of particles in a turbulent water column. MARINE ECOLOGY PROGRESS SERIES 158, 275–281.

Ward, C.H., 2017. Habitats and biota of the Gulf of Mexico: Before the deepwater horizon oil spill, Habitats and Biota of the Gulf of Mexico: Before the Deepwater Horizon Oil Spill. Springer New York. https://doi.org/10.1007/978-1-4939-3447-8

Zodiatis, G., Drakopoulos, P., Brenner, S., Groom, S., 2005. Variability of the Cyprus warm core Eddy during the CYCLOPS project. Deep-Sea Research Part II: Topical Studies in Oceanography 52, 2897–2910. https://doi.org/10.1016/j.dsr2.2005.08.020.